# Machining metals and silicon with GHz bursts: Surprising tremendous reduction of the specific removal rate for surface texturing applications

Thomas Hirsiger[a], Markus Gafner[b], Stefan Remund[a], Michalina V. Chaja[a], Aivaras Urniezius[c], Simas Butkus[c], Beat Neuenschwander[a*]

[a]Institute for Applied Laser, Photonics and Surface technologies ALPS, and
[b]Institute for Intelligent Industrial Systems I3S, Bern University of Applied Sciences, Pestalozzistrasse 20, 3400 Burgdorf, Switzerland
[c]LIGHT CONVERSION, Keramiky Street 2B, Vilnius, LT-10233, Lithuania

## ABSTRACT

Bursts of 230 fs pulses with up to 25 pulses having a time spacing of 180 ps were applied to steel AISI304, copper DHP, brass and silicon in real surface texturing (milling) application by machining squares. The previously reported very high removal rates for GHz bursts could not be confirmed, on the contrary, the specific removal rate tremendously drops down to less than 10% for the metals and 25% for silicon when the number of pulses per burst is increased. This drop is fully in line with shielding effects already observed in case of MHz pulses and double pulse experiments. The increase of the number of pulses per burst directly goes with strongly increased melting effects which are assumed to additionally re-fill the already machined areas in this milling application. Calorimetric experiments show an increasing residual heat with higher number of pulses per burst. Further the removal rates of the GHz bursts directly follow the tendency of single pulses of identical duration. This fosters the hypothesis that in case of metals and silicon only melting and melt ejection lead to the high reported removal rates for GHz bursts in punching applications and that no additional "ablation cooling" effect is taking place.

**Keywords:** GHz bursts, laser micro-machining, fs pulses, efficiency, ultra short pulses, specific removal rate

## 1. INTRODUCTION

High throughput surface structuring with ultra-short laser pulses is still a demanding task. Especially metals show an optimum point where most volume per energy can be removed i.e. the specific removal rate shows a maximum value[1-3] going with an optimum peak fluence of $e^2$ times the threshold fluence in case of a Gaussian beam. Working at this optimum point also guarantees a high surface and machining quality, especially in case of steels, often used for industrial applications. For spot radii in the range of 10 µm – 25 µm, often used for micromachining applications, this leads to maximum pulse energies of some tens of µJ and therefore to very high repetition rates up into the range of several tens of MHz for high average powers[3,4]. In metals high repetition rates can lead to particle/plasma shielding[4,5] and in case of steel also to bumpy surfaces due to heat accumulation[6]. To avoid or reduce such effects the spot to spot overlap should be reduced resulting in very high marking speeds which are today only offered by polygon line scanners[4,7-9]. Removal rates up to 27.8 $mm^3$/min for aluminum, 21.4 $mm^3$/min for copper, 15.3 $mm^3$/min for stainless steel (AISI 304) and 129.1 $mm^3$/min for $Al_2O_3$ ceramic were achieved with an average power of 187 W and 10 ps pulse duration[8]. With an average power of 306 W and 3 ps pulse duration the removal rates for steel and copper amounted 35.4 $mm^3$/min respectively 39.5 $mm^3$/min[4]. But heat accumulation and particle/plasma shielding were still an issue and could further be reduced by introducing an interlaced mode[10] demanding even higher marking speeds and a full synchronization of the scanning device and the laser. Indeed, the removal rate for stainless steel could be increased from 15.2 $mm^3$/min to 23.3 $mm^3$/min (but not in interlaced mode) when the highest marking speed of 800 m/s was used[8].

*beat.neuenschwander@bfh.ch; phone +41 34 426 42 20; alps.bfh.ch

However, standard galvo-scanners offer much higher flexibility for micromachining applications but only limited marking speeds. Therefore, solutions for using such scanners at high average power are highly demanded. Dividing the pulse energy into several smaller sub-pulses with a time interval of some ns, i.e. introducing the burst mode, reduces the requirements for a very high repetition rate and marking speed and make bursts suitable for galvo scanning. First publications in case of ultra-short pulses denoted the bursts to be more efficient compared to single pulses[11] but the reported benefit was often only due to the reduced peak fluence of a single pulse in the burst[12]. Having a closer look reveals a more complex behavior for surface texturing with bursts. Metals like copper, brass, silver, and gold show a strong drop of the specific removal rate for a 2-pulse burst[13,14]. This strong drop is assumed to be caused by the particle/plasma shielding effect[5] an assumption which is confirmed by shadowgraphy experiments[15,16]. A complete shielding would lead to a halved value for the specific removal rate, but as the observed drop even exceeds 50% of the value for single pulses an additional effect takes place. Material re-deposition is assumed to be responsible for this high reduction which is supported by the shadowgraphy experiments and the fact that this behavior is also observed for an intra burst time interval of 60 ns[13].

For a 3-pulse burst the specific removal rate increases again almost to the value of single pulses or exceeds it by about 15% in case of copper. For the latter material this surprising behavior continues for a higher number of pulses per burst i.e. a low specific removal rate is obtained for an odd and a high value is obtained for an even number of pulses for IR and for green but, the difference between the specific removal rates decreases with increasing pulse number[14,16]. For copper the higher specific removal rate for a 3-pulse burst could be explained by an increased absorptance of the machined surface. Calorimetric experiments showed almost a doubling of the absorptance of the machined surface from about 14% for single pulses up to 27% for a 3-pulse burst[17,18] i.e. at least the first sub pulse of the 3-pulse burst sees a significantly higher absorptance finally leading to an increased removed volume going with higher specific removal rates. For steel AISI 304 these effects are almost absent or strongly reduced[12,16] but double pulse experiments demonstrated that also steel shows a strong shielding effect, but on a much shorter time scale. It is shown that the removal rate drops by about 80% for a time interval of 200 ps and restores for 20 ns and more[19].

Recently bursts with very short intra burst time intervals, so called GHz-bursts, have attracted a lot of attention. A first publication about GHz-burst with 300 fs pulses at a wavelength of 1030 nm reported specific removal rates up to approximately 7.6 $\mu m^3/\mu J$ (400 pulses at 1.728 GHz corresponding to 580 ps intra burst time interval) for copper and 13 $\mu m^3/\mu J$ (800 pulses at 3.456 GHz) for silicon[20]. The value for silicon could be improved by the same group to about 29 $\mu m^3/\mu J$ (560 pulses at 1.6 GHz)[21]. These values could even be increased to 42.2 $\mu m^3/\mu J$ for silicon (200 pulses at 0.88 GHz) for silicon[22] and 11.5 $\mu m^3/\mu J$ (200 pulses at 1.76 GHz) for copper[23]. For aluminum and stainless steel AISI 304 maximum values of 38.3 $\mu m^3/\mu J$ and 23.3 $\mu m^3/\mu J$ (200 pulses at 1.76 GHz) were presented[23]. The presented values are impressive and definitively much higher than the values of 3.1 $\mu m^3/\mu J$ and 4.4 $\mu m^3/\mu J$ obtained for copper and steel with single pulses at a repetition rate of 505 kHz and a pulse duration of 350 fs[24]. This increase is explained by the "ablation cooling" effect where most of the heat is assumed to be carried away by ablation before thermal diffusion into the material occurs[20]. A hypothesis which is also supported by a hydrodynamic two-temperature model[25]. In this work it is stated that to prevent shielding and suppression effects the fluence of each pulse in the burst should have a subthreshold value to avoid the generation of slow moving ablated condensed-phase nanolayers.

However, all the presented results are obtained for punching applications like drilling or machining of dimples, processes where also just heat accumulation combined with melt ejection could lead to an increase in the process efficiency as less material has to be evaporated. E.g. the latent heat of fusion and of vaporization for copper amounts 13.3 kJ/mol and 305 kJ/mol, respectively i.e. a process which only bases on the melt phase can be up to a factor of 23 more efficient compared to a process demanding vaporization of the material. Further it has been shown by experiments and simulations that the reported high efficiencies cannot be transferred from a punching to a milling process due to the changed melt flow in the different machining processes[26]. In contrary, this would lead to an even much larger heat accumulation without any "ablation cooling" effect. The nature of the GHz-burst machining is therefore still not clear and additional experiments are clearly needed to gain a better picture.

## 2. EXPERIMENTAL SET – UP

The used PHAROS PH1-20 laser source emitting 230 fs pulses at a wavelength of 1028 nm with repetition rates between 1 kHz and 1 MHz offered a bi – burst mode, i.e. the combination of bursts with 5.4 GHz (180 ps intra-burst time interval) and 65 MHz (15.4 ns intra-burst time interval). The maximum number of pulses per burst was limited to 25 and 8 for the GHz and the MHz burst, respectively. The energy of the single pulses in the burst in GHz – case were monitored with an ultrafast photodiode (UPD-15-IR2-FC InGaAs Photodetector) and a high bandwidth oscilloscope (LeCroy with 40 Gs/s

and 6 GHz Bandwidth). The adjustment of the energy of the single pulses in the burst sequence was restricted, only a general trend, defining an increasing or decreasing energy of the single pulses, could be set. But, for stable operation the last pulse of the burst train had to cover the remaining part of the energy stored in the regenerative amplifier. Therefore, for 4 and more pulses per burst the energy of the last pulse in the burst train was always significantly higher than the energy of the previous ones. Figure 1a shows the oscilloscope signals of the shapes set for a 2, 3, 4, 8, 6 and 25 pulse GHz – burst.

A sketch of the experimental set-up is shown in figure 1b). The laser was operated at its maximum power of about 20 W which was then adjusted by turning a half-wave plate in front of a thin film polarizer. The beam was guided via folding mirrors and a 2x Galilei – telescope to an excelli*SCAN* 14 and was then focused onto the target with either an $f$ = 100 mm telecentric or with an $f$ = 160 mm f – theta objective. The spot size and beam quality factor of the focused beam were measured with a BP-104-IR rotating slit beam analyzer at a laser repetition rate of 1 MHz. The corresponding values amounted $w_0$ = 10.4 µm with $M^2$ = 1.4 and $w_0$ = 16.2 µm with $M^2$ = 1.35 for the $f$ = 100 mm and the $f$ = 160 mm objective, respectively. The scanner was fully synchronized[27, 28] to the PHAROS laser system to guarantee highest precision.

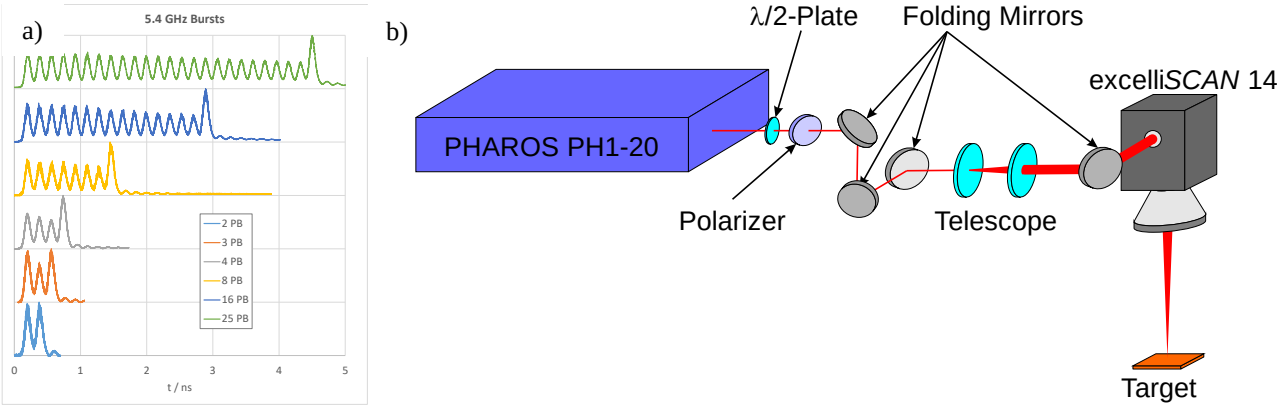


Figure 1. a) Oscilloscope signals of the GHz – bursts with 2, 3, 4, 8, 16 and 25 pulses. b) Sketch of the experimental set – up.

The specific removal rate $\gamma_{spec}$ i.e. the removed volume per energy or the removal rate per average power was deduced for GHz bursts with $n_b$ = 1, 2, 3, 4, 8, 16 and 25 pulses per burst. As example of a real surface texturing application, a series of squares with a side length of $s$ = 1 mm were machined into copper DHP, brass, steel AISI304, brass and silicon with the $f$ = 160 mm objective and a repetition rate of $f_{rep}$ = 100 kHz. For silicon additional experiments were done with the MHz burst. For defined and reproducible starting conditions the surface of the metal targets with a dimension of 50x50mm and a thickness of 2 mm was lapped whereas the silicon target with the same size was cut out from a (100) single side polished p – type wafer of 650 µm thickness and having a surface resistance of $\rho = 1 - 100\ \Omega \cdot cm$. The average power $P_{av}$ i.e. the peak fluence $\phi_0$ of the individual pulses in the burst was increased from square to square from values below the threshold to several $J/cm^2$ or in case of higher number of pulses per burst the maximum average power if it was already reached at lower fluences. The spot to spot distances in scan and cross-scan direction were set to $p_x = p_y$ = 8 µm corresponding to an overlap of about 75 %. The number of repetitions $n_r$ was chosen accordingly to obtain a constant number of individual pulses per area i.e. $n_b \cdot n_r$ amounted 192 for steel and 96 for all other materials. Only for the 25 pulse burst this condition could not be fulfilled and the corresponding numbers amounted 200 and 100. The samples were cleaned in an ultrasonic bath with Alconox® and the depth $d$ of the squares and the surface roughness $s_a$ were measured with an interferometric white – light microscope smartWLI from gbs. The specific removal rate is given by:

$$\gamma_{spec} = \frac{p_x \cdot p_y \cdot d \cdot f_{rep}}{n_b \cdot n_r \cdot P_{av}} \tag{1}$$

To verify the hypothesis of ablation cooling the energy remaining in the material $E_{res}$ during machining, the residual heat, was deduced for copper with additional calorimetric experiments[6, 18]. For this special cooling effect most of the heat is assumed to be carried away by ablation before its thermal diffusion into the material[20]. This should lead to a reduction of the residual heat and therefore al lower fraction $\eta_{res} = E_{res}/E_{in}$ when the material is machined with GHz bursts.

For a Gaussian beam the specific removal rate and many other measures are in general presented as a function of the peak fluence. For the burst situation with varying pulse energy of the individual pulses this value means its average which is given by:

$$\phi_0 = \frac{2 \cdot P_{av}}{f_{rep} \cdot \pi \cdot w_0^2 \cdot n_b} \tag{2}$$

# 3. EXPERIMENTAL RESULTS

## 3.1 Machined squares

The obtained results for the squares machined into copper are summarized in figure 2. Up to 16 pulses per burst the removal rate tremendously drops with increasing number and then very slightly increases for the 25 pulses per burst (figure 2a). The specific removal rate as a function of the peak fluence of an individual sub pulse is shown in figure 2b and table 1. Its maximum value dramatically drops from 3.12 µm³/µJ down to 0.24 µm³/µJ and 0.3 µm³/µJ for the 16 and the 25 pulse burst which is less than 10% of the value obtained for a 1 pulse burst. The surface roughness value $s_a$ in dependence on the specific removal rate is finally presented in figure 2 c. For all burst situations the surface roughness first increases with the specific removal rate up to its maximum value. This represents the first part up to the optimum fluence with the maximum specific removal rate in figure 2b. For higher fluences where the specific removal rate starts to drop the surface roughness further increases, i.e. a quite good surface quality is obtained at the optimum point. For a 2, 3, 4 or 8 pulse burst the surface at the highest specific removal rate is always rougher than the one obtained for the 1 pulse burst at identical specific removal rate. Only for very low specific removal rates bursts can lead to lower roughness values compared to the 1 pulse situation.

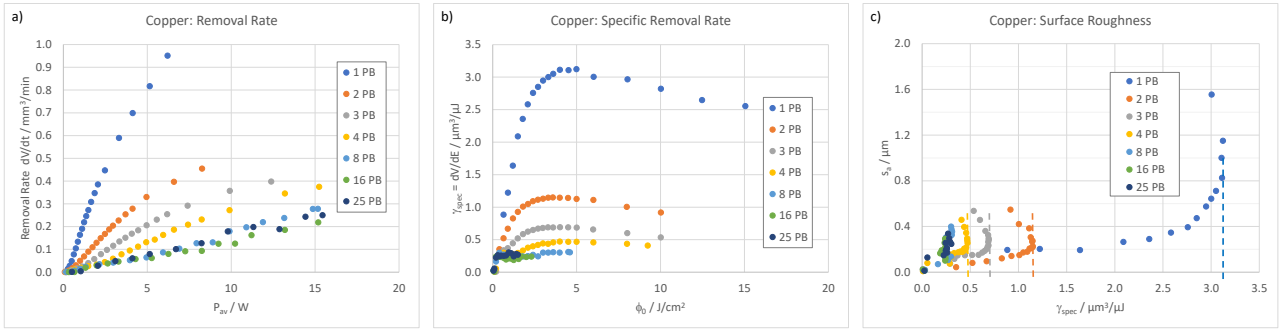


Figure 2. Results for the squares machined into copper with GHz – bursts and up to 25 pulses per burst: a) Removal rate as a function of the average power. b) Specific removal rate as a function of the sub – pulse mean peak fluence. c) Surface roughness dependent on the achieved specific removal rate.

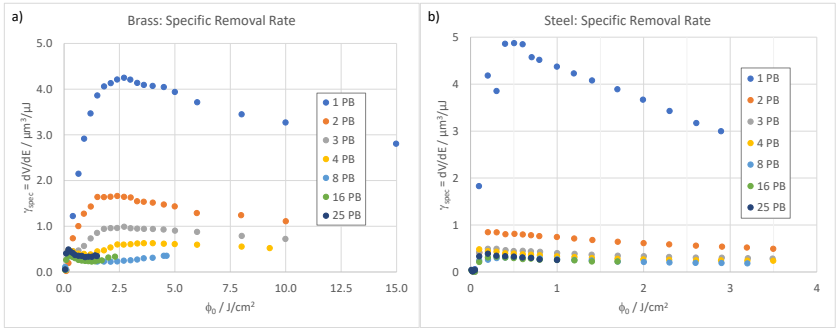


Figure 3. Specific removal rates as a function of the peak fluence of the individual pulses for the squares machined into brass a) and steel b) with GHz – bursts and up to 25 pulses per burst.

A similar behavior is also observed for steel and brass. The specific removal rates are shown in figure 3 and the corresponding maximum values are summarized in table 1. The lowest maximum specific removal rate is obtained for the 8 pulse burst where it dropped, compared to the value of a 1 pulse burst, to 8% and 6% for brass and steel. These maximum

values then slightly increases to 12% and 8% for the 25 pulse burst, but are still about 10 times lower than the ones for a 1 pulse burst.

For silicon the drop in both removal rates, shown in figure 4a and b, is less pronounced. For the 3, 4, 8 and 16 pulse burst the specific removal rate drops by about 75% compared to the value obtained for the 1 pulse burst which is significantly less than the maximum values of more than 90% observed for the investigated metals. For the 25 pulse burst the maximum specific removal rate then increases to 36% of the value for single pulses, which is the highest value of all four materials for the 25 pulse burst. Except for the 2 pulse burst the highest specific removal rate is observed at the highest applied peak fluence i.e. no optimum point exist and the specific removal rate seems to grow with the applied peak fluence. A different behavior is also observed for the surface roughness where in general the value increases with the specific removal rate as shown in figure 4c.

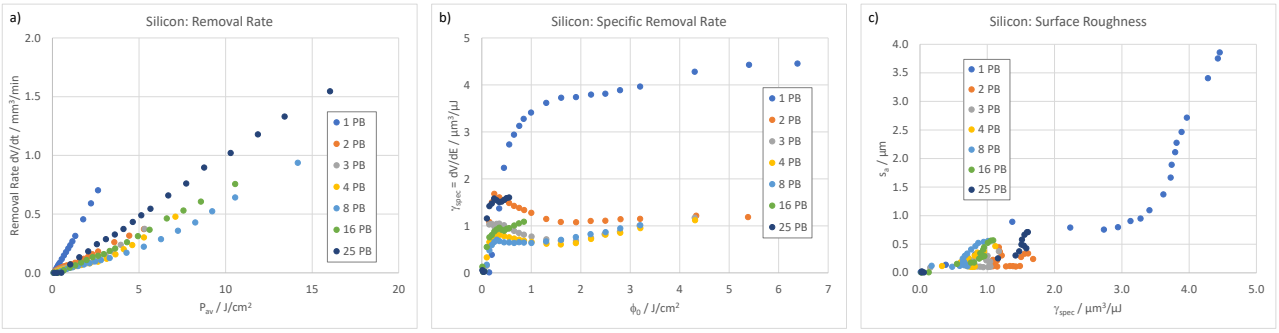


Figure 4. Results for the squares machined into silicon with GHz – bursts and up to 25 pulses per burst: a) Removal rate as a function of the average power. b) Specific removal rate as a function of the sub – pulse mean peak fluence. c) Surface roughness dependent on the achieved specific removal rate.

The maximum specific removal rates (absolute and relative) and the corresponding surface roughness values are all summarized in table 1. The values imply that a lower roughness value is achieved with GHz bursts but one has to have in mind that the corresponding removal rates are significantly lower and that for many situation the 1 pulse burst at identical specific removal rate would lead to even lower roughness values.

Table 1. Maximum specific removal rates and observed surface roughness values for all four investigated materials

| #pulses | 1 | 2 | 3 | 4 | 8 | 16 | 25 |
|---|---|---|---|---|---|---|---|
| Copper $\gamma_{max}$ | 3.12 µm³/µJ | 1.15 µm³/µJ | 0.69 µm³/µJ | 0.47 µm³/µJ | 0.31 µm³/µJ | 0.24 µm³/µJ | 0.3 µm³/µJ |
| $\gamma_{max,rel}$ | 100% | 37% | 22% | 15% | 10% | 8% | 10% |
| $s_a$ | 1.15 µm | 0.23 µm | 0.2 µm | 0.26 µm | 0.35 µm | 0.12 µm | 0.25 µm |
| Brass $\gamma_{max}$ | 4.25 µm³/µJ | 1.66 µm³/µJ | 0.99 µm³/µJ | 0.63 µm³/µJ | 0.35 µm³/µJ | 0.36 µm³/µJ | 0.49 µm³/µJ |
| $\gamma_{max,rel}$ | 100% | 39% | 23% | 15% | 8% | 9% | 12% |
| $s_a$ | 0.47 µm | 0.24 µm | 0.29 µm | 0.27 µm | 0.42 µm | 0.14 µm | 0.17 µm |
| Steel $\gamma_{max}$ | 4.87 µm³/µJ | 0.85 µm³/µJ | 0.50 µm³/µJ | 0.48 µm³/µJ | 0.31 µm³/µJ | 0.33 µm³/µJ | 0.39 µm³/µJ |
| $\gamma_{max,rel}$ | 100% | 17% | 10% | 10% | 6% | 7% | 8% |
| $s_a$ | 0.27 µm | 0.13 µm | 0.12 µm | 0.12 µm | 0.23 µm | 0.25 µm | 0.25 µm |
| Silicon $\gamma_{max}$ | 4.46 µm³/µJ | 1.68 µm³/µJ | 1.17 µm³/µJ | 1.12 µm³/µJ | 1.01 µm³/µJ | 1.09 µm³/µJ | 1.60 µm³/µJ |
| $\gamma_{max,rel}$ | 100% | 38% | 26% | 25% | 23% | 24% | 36% |
| $s_a$ | 3.86 µm | 0.24 µm | 0.38 µm | 0.47 µm | 0.56 µm | 0.57 µm | 0.71 µm |

Micrographs of the machined squares for four different fluences and all investigated number of pulses per burst for steel are shown in figure 5. The increase in the number of pulses per burst comes along with a strong thermal coloring i.e. an oxidation of the surface and increased debris around. A similar behavior is observed for copper, brass and concerning the debris also for silicon. The latter shows a strong formation of cone like protrusions (CLP)[29] for single pulses as illustrated by SEM micrographs in figure 6 for a peak fluence of 0.75 J/cm². The CLP's disappear for 2 and all higher number of pulses per burst due to melting effects which are increasing with the number of pulses per burst. CLP formation is also observed for steel and fluences above 1.0 - 1.5 J/cm². Again, the GHz bursts lead to increased melting effects suppressing the formation of CLP's as illustrated for a peak fluence of 3.5 J/cm² and up to 8 pulses per burst in figure 7. But this suppression of the CLP formation goes with a dramatic reduction of the specific removal rate (see table 1) for silicon and steel as well. The strong increase of melting effects is also observed for copper and brass where no formation of CLP

occurred. A detailed analysis of the surface morphology reveals an interesting behavior which is illustrated in figure 8 for steel at a peak fluence of 0.4 J/cm$^2$ corresponding to the optimum point for the 1 pulse burst. For a 1 pulse burst the surface shows typical melt worm with dimensions of µm covered by round particles of 100 nm diameter and less. For the 2 pulse burst the melt worms disappear and the surface consist of plate like structures also covered by round particles whose dimensions are slightly smaller than for the 1 pulse burst. For a higher number of pulses per burst the diameter of these particles is further reduced and the melted surface seems to become covered by particles smaller than 10 nm which are sintered and start to form a porous surface. This effect becomes more pronounced for a higher number of pulses per burst and is also observed for copper, brass and silicon.

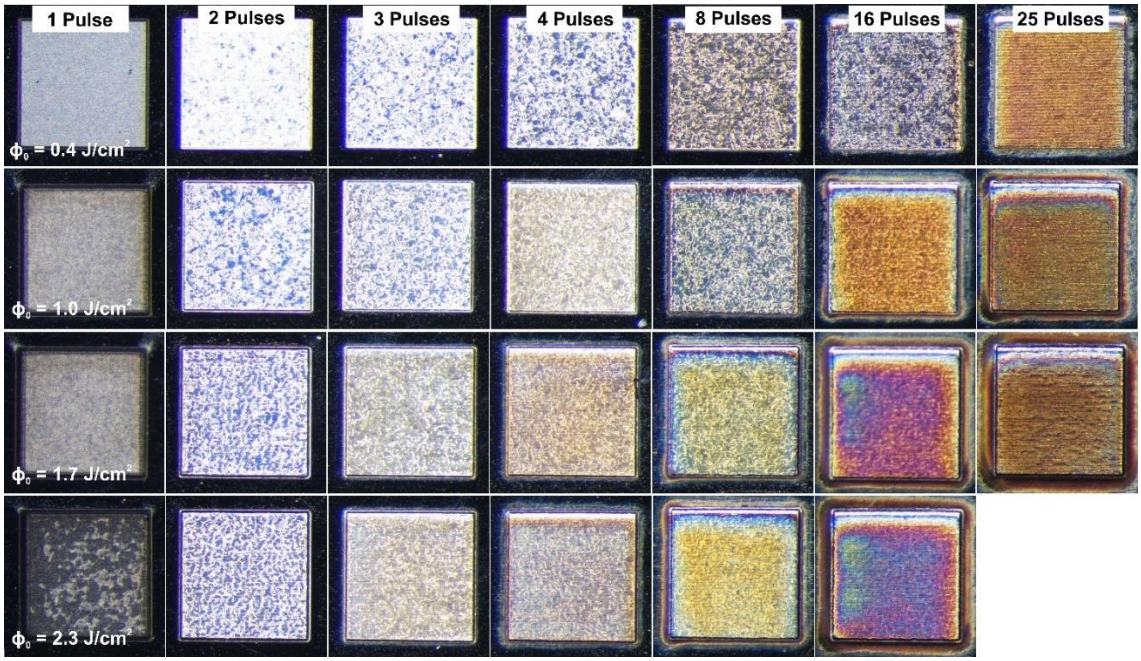


Figure 5. Micrographs of the machined squares in steel at four different peak fluences. The lowest peak fluence of 0.4 J/cm$^2$ denotes the optimum value. For all squares in one line the total energy i.e. the sum of the energy of all impinging laser pulses did not change .

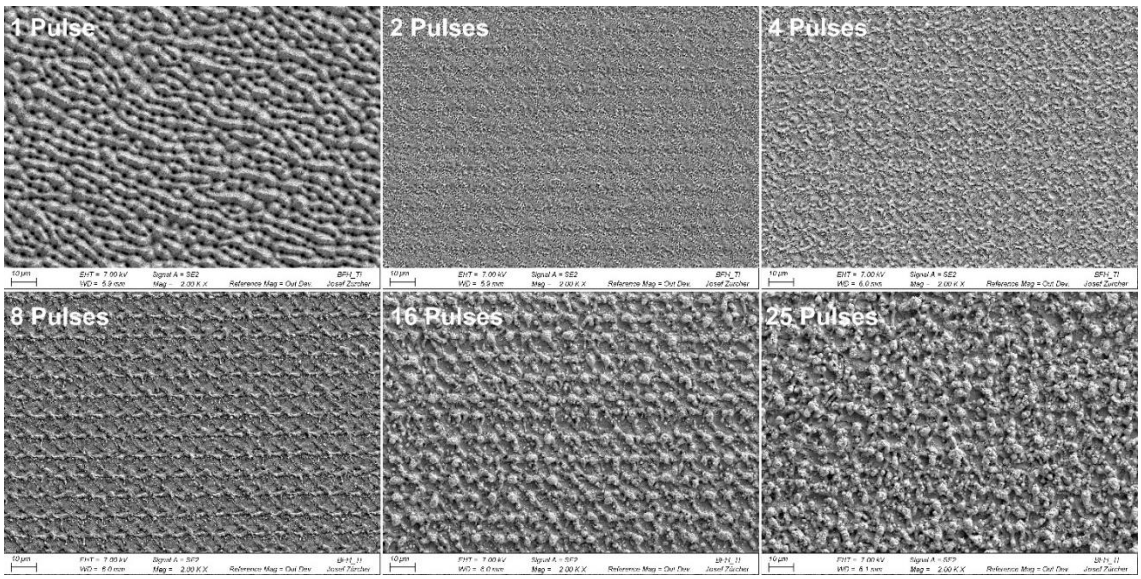


Figure 6. SEM Micrographs of the machined squares in silicon at a peak fluence of 0.75 J/cm$^2$ and 1, 2, 4, 8, 16 and 25 pulses per burst.

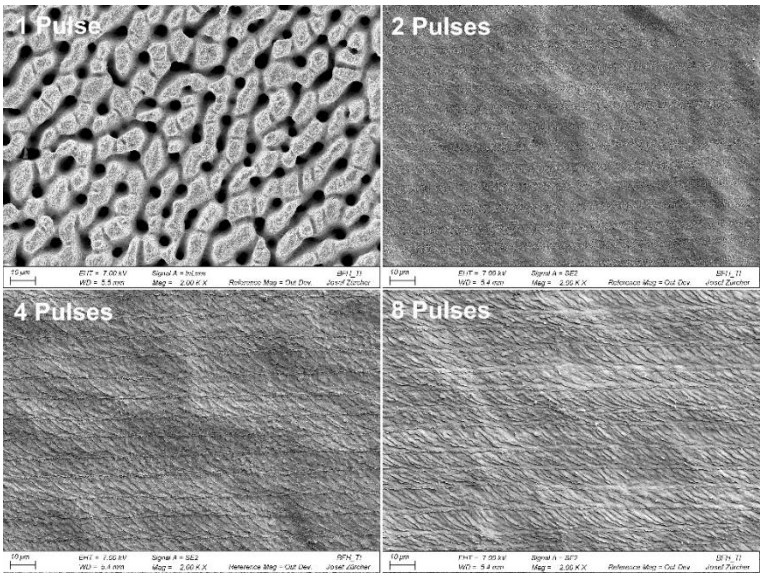


Figure 7. SEM Micrographs of the machined squares in steel at a peak fluence of 3.5 J/cm$^2$ and 1, 2, 4 and 8 pulses per burst.

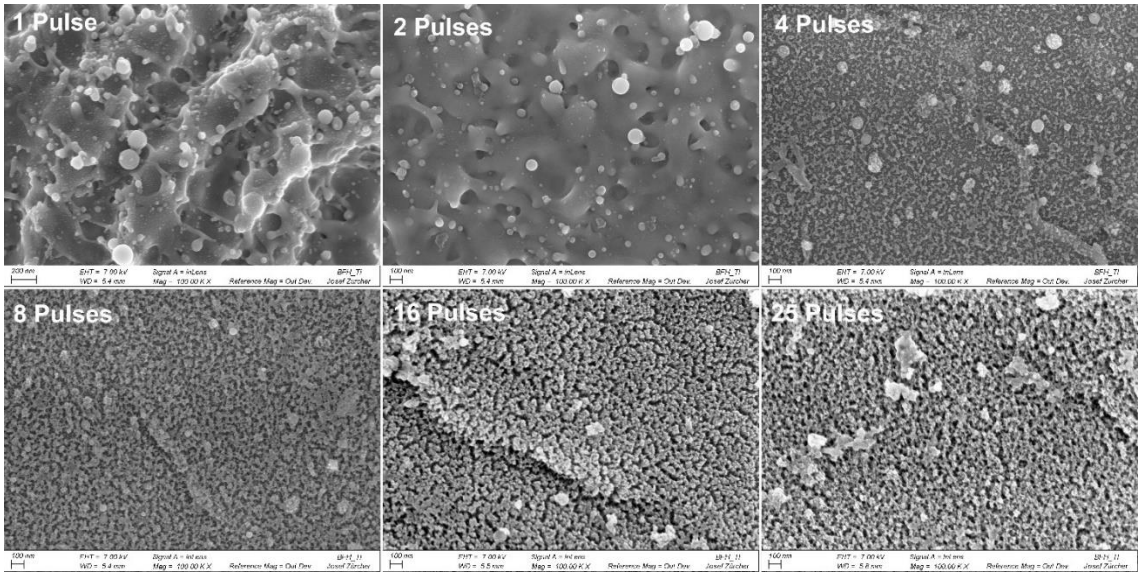


Figure 8. SEM Micrographs with high magnification of the machined squares in steel at a peak fluence of 0.4 J/cm$^2$ and 1, 2, 4, ,8, 16 and 25 pulses per burst.

### 3.2 Residual Heat

The fraction $\eta_{res}$ of the incoming energy remaining in the copper sheet during machining as a function of the number of pulses per burst for six different peak fluences ranging from 1.4 J/cm$^2$ up to 10 J/cm$^2$ is shown in figure 9. For the lower three peak fluences the $f$ = 160 mm objective was used whereas the higher three peak fluences were realized with the $f$ = 100 mm objective. For the 1 pulse burst about 25% of the incoming energy remains in the copper sheet for all investigated peak fluences. This amount then rises to 30% - 35% for increasing number of pulses per burst. For the lowest

peak fluences of 1.4 J/cm$^2$ and 2.0 J/cm$^2$ the residual heat shows the tendency of a very small decrease when the number of pulses per burst is increased from 8 to 16 and 25.

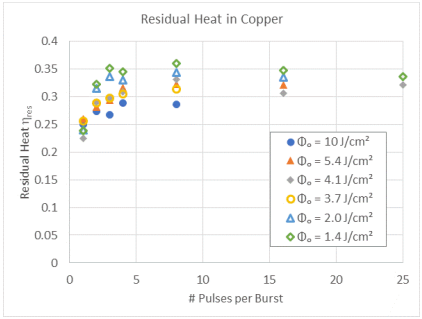


Figure 9: Residual heat during machining squares in copper for 6 different peak fluences as a function of the number of pulses per burst.

## 4. DISCUSSION

For all investigated materials a tremendous drop in the specific and in the removal rate as well is observed when they are machined with GHz-bursts and up to 25 pulses per burst. For a 2 pulse burst the measured drop for copper can directly be compared with double pulse experiments[15] with varying time spacing between the two pulses. There, a drop of the ablation depth for the machined squares from about 60 µm down to 24 µm and 22 µm was reported for a time spacing of 0 ps, 110 ps and 250 ps at a peak fluence of about 1.4 J/cm$^2$ for each pulse. For the time spacing of 0 ps the two pulses coincide resulting in one pulse with doubled peak fluence. As the ablation depth directly scales with the specific removal rate these values can be compared with the actual rates at similar peak fluences amounting 2.7 J/cm$^2$ for the 1 pulse burst and 1.5 J/cm$^2$ otherwise. Here a drop from 2.85 µm$^3$/µJ down to 0.93 µm$^3$/µJ was observed. The relative drops therefore amount about 60 % for the double pulse experiments and 67 % for the 2 pulse burst (having a time spacing of 180 ps). Similar pump-probe experiments are presented for steel 1.4301 and silicon[19]. The drops for a time spacing of about 200 ps amounted about 75% for steel at a peak fluence of 1 J/cm$^2$ and 67% for silicon at a peak fluence of 1.4 J/cm$^2$. The 2 pulse burst experiments showed drops of 80% for steel and 70% for silicon at corresponding peak fluences. All these measured drops are of the same order and confirm a strong expanding dens plasma or particle plume leading to a strong shielding effect which was predicted[5].

In contrast to 40 MHz and 80 MHz bursts where for copper and brass a high maximum specific removal rates for an odd and a low ones for an even number of pulses per burst were observed[13-16,30] this effect is completely absent for GHz bursts as illustrated in figure 10a. For a fixed peak fluence the specific removal rate tremendously drops up to the 4 pulse burst. It then starts to increase for silicon and further drops and stays low for all three metals. Assuming a complete shielding of the second and each subsequent pulse of burst, the relative specific removal rate would read $\gamma_{spec,n}/\gamma_{spec,1} = 1/n$ with n the number of pulses per burst, represented by the dotted black line in figure 10a. If the measured value is above this line at least one of the subsequent pulses contributes to the material removal process. If the measured value is lower the subsequent pulses even hinders the material removal process of the first pulse of the burst sequence i.e. they re-deposit material[15]. For all materials the measured values are first below this value and the removal process of the first pulse is hindered. Complete shielding is reached after about 6 pulses for silicon, around 10 pulses for copper and 16 pulses for brass and steel. Only if the number of pulses per burst exceeds these values the subsequent pulses start to contribute to the material removal process. But even this contribution would finally exceed the one of the first pulse, the specific removal rate would only slowly recover as the negative influence of the first subsequent pulses has to be compensated. For silicon and assuming a linear increase, based on the results for the 8, 16 and 25 pulse burst, "break even" i.e. $\gamma_{spec,n}/\gamma_{spec,1} = 1$ would be achieved for more than 50 pulses per burst, corresponding to a burst duration of about 9 ns. The identical calculation leads to about 200 pulses for steel and 160 pulses for copper and brass corresponding to 36 ns and 30 ns until “break even” would be reached. Measurements with higher numbers of pulses per burst are demanded to clarify if this assumption of a linear increase of $\gamma_{spec,n}/\gamma_{spec,1}$ holds. However, these considerations clearly show that a high number of pulses per burst going with a long burst duration is supposed to be needed to achieve the same specific removal rate than for a 1 pulse burst. Further, for silicon MHz bursts lead to an increase in the maximum specific removal rate as well as shown in figure 10b. Thus, an advantage of GHz bursts compared to MHz bursts, if it really exists, would then be obtained far above 50 pulses per burst in the GHz case.

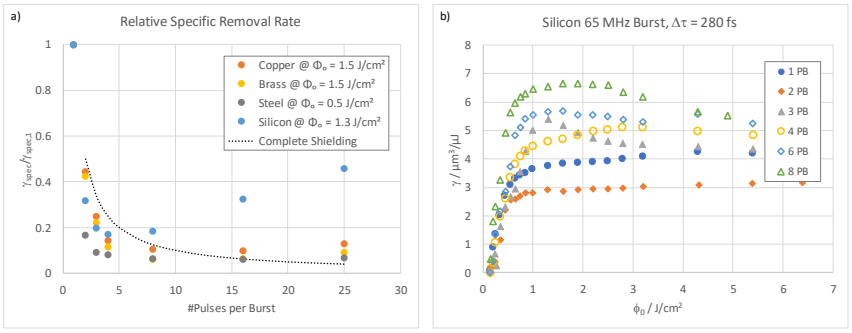


Figure 10: a) Relative specific removal rate for GHz bursts as a function of the number of pulses per burst. The black dotted line represents complete shielding of the subsequent pulses. For values below this line the material removal from the first pulse is hindered whereas for values above this line at least one of the subsequent pulses contributes to the material removal process. b) Specific removal rate for silicon and MHz bursts as a function of the peak fluence and the number of pulses per burst.

The complete shielding in figure 10a, which is supposed to be passed for copper around 10 pulses per burst for a peak fluence of 1.5 J/cm$^2$, reveals an interesting detail. For a comparable peak fluence of 1.4 J/cm$^2$ the residual heat seems to reach its maximum around 8 pulses per burst and then very slightly decreases for 16 and 25 pulses as shown in figure 9. This implies that the residual heat is increasing due to the push back and re-deposition of material removed by the first pulse until the point of complete shielding with no re-deposited material is reached. For a higher number of pulses per burst the energy of the additional subsequent pulses is then partially converted into the material removal process and the residual heat starts to slightly decrease. This hypothesis should be fostered by additional measurements with higher number of pulses per burst.

The deduction of the threshold fluence $\phi_{th,0}$ from the measured specific removal rates is rather inaccurate due to the measurement errors of the square depth which is less than 1 µm around this point. But a tendency to a significantly lower value for increasing number of pulses per burst can be observed. For copper and steel the threshold fluence drops from about 0.35 J/cm$^2$ and 0.05 J/cm$^2$ for the 1 pulse burst below 0.1 J/cm$^2$ and 0.03 J/cm$^2$ for the 25 pulse burst. This tendency has also been observed[20] for GHz bursts and copper with 800 and 400 pulses per burst, as shown in figure 11a. There the specific removal rates deduced from the results presented in [20] are plotted for a 3.46 GHz burst with 800 pulses and a 1.73 GHz burst with 400 pulses. Additionally, the specific removal rates of the actual experiments with a 1 pulse burst are shown. With a maximum of 3.1 µm$^3$/µJ these rates are significantly lower than the ones presented in[20] going up to about 8 µm$^3$/µJ. If vaporization is assumed for the material removal process the demanded energy per unit volume assuming a completely molten state at 1358 K as starting point, a vaporization temperature of 2870 K, a specific heat capacity of 385 J/kg/K and a specific vaporization enthalpy of 4'730 kJ/kg would amount 0.0473 µJ/µm$^3$. Ellipsometry showed a reflectivity of $R_s$ = 0.966 for a polished copper surface. For the liquid state n and k slightly above the melting temperature were measured with high temperature ellipsometry[31] resulting in a reflectivity of $R_l$ = 0.94. From the calorimetric experiments it is known that the reflectivity of a machined surface is lower and amounts about $R_{eff,s}$ = 0.55 for the 25 pulse burst. From this the reflectivity of the molten surface can be estimated by $R_{eff,l} = R_{eff,s} * R_l / R_s$=0.438. But for a Gaussian beam, assuming an exponential drop of the deposited energy with the depth z a maximum part of $2/e^2$ = 0.27 (factor in eq. 5 in [3]) of the energy can really be transferred to removed material. Taking all this into account the demanded energy per unit volume for vaporization raises up to 0.311 µJ/µm$^3$ or a maximum volume of 3.21 µm$^3$ per µJ of incoming energy could be evaporated. This value is represented by the dashed line in figure 11a. For specific removal rates above this values a part of the removed material is removed by melt ejection and is not vaporized. This part increases with the difference to the vaporization value implying that the presented high removal rates for GHz bursts are obtained by increased melt ejection where much less energy per volume is needed compared to vaporization.

The previous calculation, even it might be inaccurate, clearly shows that increased melt ejection could be responsible for the reported high removal rates in case of GHz bursts[20-23] and no "ablation cooling" effect is taking place. This would also explain the lower threshold fluences obtained for GHz bursts and is further fostered by the SEM micrographs in figure 6, 7 and 8 for silicon and steel where increased melting effects with increased number of pulses per burst can be observed. Already for a 2 pulse burst melting effects avoid the CLP formation and these melting effects increases with the number of pulses per burst for all investigated materials.

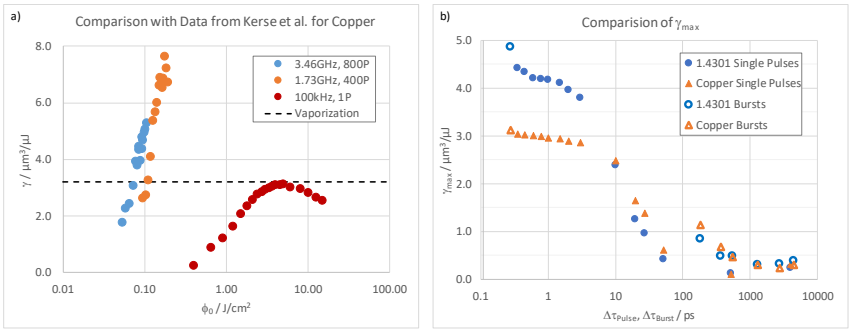


Figure 11. a) Deduced specific removal rate from [20] as a function of the peak fluence for 1.73 GHz and 400 pulses per burst, 3.64 GHz and 800 pulses per burst compared to the actual results with a 1 pulse burst. The black dashed line denotes the maximum volume that can be evaporated per energy. b) Maximum specific removal rate for steel and copper as a function of the burst duration (GHz bursts) and pulse duration (single pulses).

Further, a higher amount of ejected melt, would have a higher influence onto punching compared to milling applications where the melt will "re-fill" the just machined part of the surface as also shown in[25]. From the micrographs in figure 5 it is obvious that the burr and debris around the squares is increasing with the peak fluence and the number of pulses per burst. In figure 12 horizontal line profiles around the square edge for the peak fluence of 1 J/cm$^2$ (2$^{nd}$ line in figure 5) are shown. The burr height is generally increasing with the number of pulses per burst even the total energy per area did not change further fostering the hypothesis that a higher number of pulses per burst leads to an increased melt ejection.

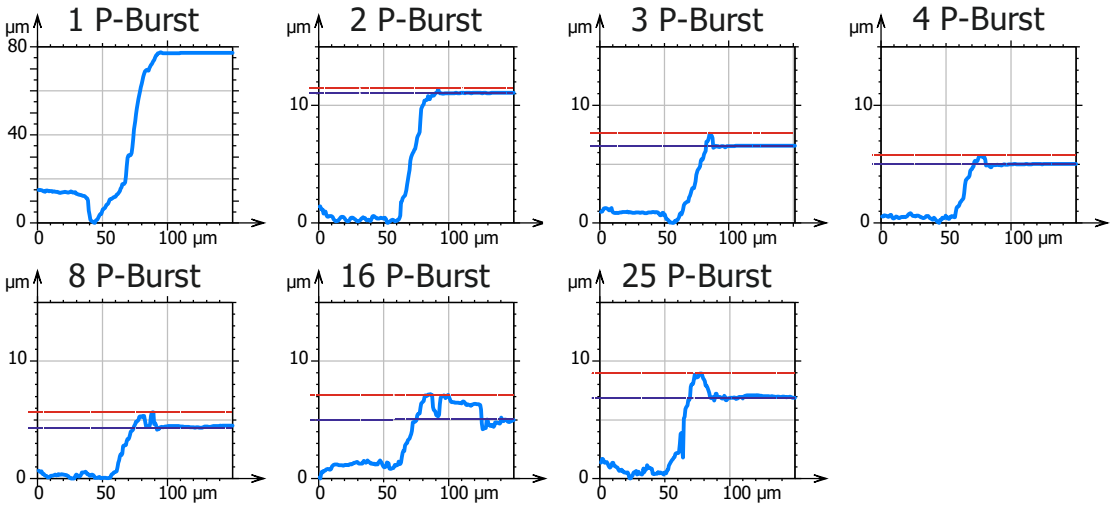


Figure 12. Horizontal line profiles around the edges of the squares machined in steel with a peak fluence of 1 J/cm$^2$. The blue dotted line denotes the level of the original surface and the red dotted line the top of the burr.

In figure 11b the maximum specific removal rates as a function of the burst duration are compared with 1 pulse bursts (single pulses) of different pulse durations from former experiments. The maximum rates clearly follow the same tendency, they first slightly drop up to a duration of a few ps, followed by a strong decrease up to several 100 ps and a slow recovery into the low ns range. For punching application (drilling) GHz bursts were compared with ns-pulses[23]. For copper a maximum specific removal rate of 11.7 µm$^3$/µJ for a 1.76 GHz burst of 113ns duration was reported. This value is very near the 10 µm$^3$/µJ obtained for a 100 ns pulses. For steel AISI 316L the corresponding values amount 23.3 µm$^3$/µJ and 30 µm$^3$/µJ for the GHz burst and the ns pulses, respectively. This clearly shows that the removal rates of GHz bursts are directly following the ones of single pulses (1 pulse bursts) of identical duration. Further experiments are needed to exactly compare the machining quality of the GHz bursts and the ns pulses.

## 5. CONCLUSION

GHz bursts with up to 25 pulses per burst were applied to steel AISI304, copper DHP, brass and silicon in real surface structuring (milling) application by machining squares. For this application the previously reported very high removal rates could not be confirmed, on the contrary, the specific removal rate tremendously drops down to less than 10% for the metals and 25% for silicon when the number of pulses per burst is increased. This drop is fully in line with shielding effects, already observed in case of MHz pulses and double pulse experiments, dominating the material removal process of the first pulses of the burst and leading to a slow recovery of the specific removal rate with further increase of the number of pulses per burst. Optical and SEM microscopy showing strong melting effects as well as calculations concerning the energy needed to evaporate material indicate that the reported high removal rates for GHz bursts in punching applications are reached because material is only melted and ejected which is much less energy consuming than a vaporization. In milling applications this melted material is assumed to "re-fill" the machined area which is additionally reducing the specific removal rate. Further it can be seen that the measured maximum specific removal rates of GHz bursts with different durations i.e. number of pulses per burst follow the trend of single pulses (1 pulse bursts) of corresponding duration. This supports the hypothesis that for metals and silicon GHz burst acts like single pulses of corresponding duration and that melt ejection processes and not the postulated "ablation cooling" process are responsible for the high removal rates reported for punching applications.

However, it has to be clarified if GHz bursts lead to a higher machining quality compared to single pulses and how they behave in case of ceramics or glasses/crystals with a high bandgap. For the latter the generation of excited states with the first pulses in the burst could lead to a different behavior of the material to be machined.


## ACKNOWLEDGEMENTS

The authors wish to thank Joseph Zuercher and Patrick Neuenschwander for their help with the WLI and SEM microscopy.


## REFERENCES


[1] Furmanski, J., Rubenchick, A. M., Shirk, M. D. and Stuart, B. C., "Deterministic processing of alumina with ultrashort pulses," Journal of Appl. Phys 102, 073112 (2007)

[2] Raciukaitis, G., Brikas, M., Gecys, P., Voisiat, B., Gedvilas, M., "Use of high repetition rate and high power lasers in microfabrication: How to keep the efficiency high?," JLMN Journal of Laser Micro/Nanoengineering 4, 186 (2009)

[3] Neuenschwander, B., Jaeggi, B., Schmid, M., Hennig, G., "Surface Structuring with ultra-short laser pulses: Basics, limitations and needs for high throughput," Phys. Proceedia 56, 1047 – 1058 (2014)

[4] Jaeggi, B., Remund, S. M., Streubel, R., Goekce, B., Barcikowski, S., Neuenschwander, B., "Laser Micromachining of Metals with Ultra-Short Pulses: Factors Limiting the Scale-Up Process," Journal of Laser Micro/Nanoengineering 12, 267 – 273 (2017)

[5] Koenig, J., Nolte, S. and Tuennermann, A., "Plamsa evolution during metal ablation with ultrashort pulses," Optics Express 13, 10597 – 10607 (2005)

[6] Bauer, F., Michalowski, A., Kiedrowski, T. and Nolte, S., "Heat accumulation in ultra-short pulsed scanning laser ablation of metals," Optics Express 23, 1035 – 1043 (2015)

[7] Jaeggi, B., Neuenschwander, B., Zimmermann, M., Pennig, L., deLoor, R., Weingarten, K. and Oehler, A., High Throughput and High Precision Laser Micromachining with ps-Pulses in Synchronized Mode with a fast Polygon Line Scanner," Proc. of SPIE 8967, 89670Q (2014)

[8] Schille, J., Schneider, L., Streek, A., Kloetzer, S. and Loeschner, U., "High-throughput machining using a high-average power ultrashort pulse laser and high-speed polygon scanner," Optical Engineering 55, 096109 (2016)

[9] Loeschner, U., Schille, J., Streek, A., Knebel, T., Hartwig, L., Hillmann, R. and Endisch, Ch., "High-rate laser microprocessing using a plygon scanner system," Journal of Laser Applications 27, S29303 (2015)

[10] Neuenschwander, B., Jaeggi, B., Zimmermann, M., Markovic, V., Resan, B., Weingarten, K., deLoor, R. and Pennig, L., "Laser surface structuring with 100W of average power and sub-ps pulses," 34th International Congress on Applications of Lasers & Electro-optics ICALEO, M102 (2015)
[11] Knappe, R., Haloui, H., Seifert, A., Weis and A., Nebel, A., "Scaling ablation rates for picosecond lasers using burst micromachining," Proc. of SPIE 7585, 75850H (2010)
[12] Neuenschwander, B., Kramer, T., Lauer, B. and Jaeggi, B., "Burst mode with ps- and fs-pulses: Influence on the removal rate, surface quality and heat accumulation," Proc. of SPIE **9350**, 93500U (2015)
[13] Kramer, T., Zhang, Y., Remund, S., Jaeggi, B., Michalowski, A., Bauer, F. and Neuenschwander, B., " Increasing the Specific Removal Rate for Ultra Short Pulsed Laser-Micromachining by Using Pulse Bursts," JLMN Journal of Laser Micro/Nanoengineering **12**, 107 – 114 (2017)
[14] Jaeggi, B., Remund, S., Zhang, Y., Kramer, T. and Neuenschwander, B.,"Optimizing the Specific Removal Rate with the Burst Mode Under Varying Conditions," JLMN Journal of Laser Micro/Nanoengineering **12**, 258 – 266 (2017)
[15] Foerster, D. J., Faas, S., Groeninger, S., Bauer, F., Michalowski, A., Weber, R. and Graf, T., "Shielding effect and re-deposition of material during processing of metals with burts of ultra-short laser pulses," Appl. Surf. Sci **440**, 926 – 931 (2018)
[16] Bornschlegel, B. and Finger, J., "In-Situ Analysis of Ultrashort Pulsed laser Ablation with Pulse Bursts," JLMN Journal of Laser Micro/Nanoengineering **14**, 88 – 94 (2019)
[17] Jaeggi, B., Foerster, D. J., Weber, R. and Neuenschwander, B., "Residual heat during laser ablation of metals with bursts of ultra-short pulses," Adv. Opt. Technol. **7**, 175–182 (2018)
[18] Neuenschwander, B., Jaeggi, B., Foerster, D. J., Kramer, T. and Remund, S., "Influence of the burst mode onto the specific removal rate for metals and semiconductors," Journal of Laser Applications **31**, 022203 (2019)
[19] Bauer, F., "Grundlegende Untersuchungen zum Abtragen von Stahl mit ultrakurzen Laserpulsen," PhD Thesis Friedrich-Schiller-Universitaet Jena, (2018)
[20] Kerse, C., Kalaycioglu, H., Elahi, P., Cetin, B., Kesim, D. K., Akcaalan, Ö., Yavas, S., Asik, M.D., Öktem, B., Hoogland, H., Holzwarth, R. and Ömer – Ilday, F.,"Ablation-cooled material removal with ultrafast bursts of pulses," Nature **532**, 84 – 89 (2016)
[21] Elahi, P., Akcaalan, Ö., Ertek, C., Koray, E., Ömer – Ilday, F. and Kalaycoglu, H., "High-power Yb-based all-fiber laser delivering 300 fs pulses for high-speed ablation-cooled material removal," Optics Letters **43**, 535 – 538 (2019)
[22] K. Mischik et al, "High-efficiency femtosecond ablation of silicon with GHz repetition rate laser source," Opt. Let. **44**, 2193-2196 (2019)
[23] G. Bonamis et al, "High efficiency femtosecond laser ablation with gigahertz level bursts," J. Laser Appl. **31**, 022205 (2019)
[24] B. Jaeggi et al, "Influenec of the pulse duration and the experimental approach onto the specific removal rate for ultra-short-pulses," Proc. of SPIE **10091**, 100910J (2017)
[25] Povarnitsyn, M. E., Levashov, P. R. and Knyazev, D. V., "Sumulation of ultrafast bursts of subpicosecond pulses: In pursuit of efficiency," Appl. Phys. Lett. **112**, 051603 (2019)
[26] L. Zhibin et al, "ESI, ultrafast laser ablation of copper with GHz-bursts," Proc. of SPIE **10519**, 1051902 (2018)
[27] Jaeggi, B., Neuenschwander, B., Hunziker, U., Zuercher, J., Meier, Th., Zimmermann, M., Selbmann, K-H., Hennig, G., "High precision surface structuring by synchronizing a galvo scanner with an ultra short pulsed laser system in MOPA arrangement," Proc. of SPIE 8243, 82430K (2012)
[28] Jaeggi, B., Neuenschwander, B., Zimmermann, M., Zecherle, M., Boeckler, E.W. ,"Time-optimized laser micromachining by using a new high dynamic and high precision galvo scanner,", Proc of SPIE 9735, 973513 (2016)
[29] Tsukamoto, M., Kayahara, T., Nakato, H., Hashida, M., Katto, M., Fujita, M., Tanaka, M. Abe, N., "Microstructures formation on titanium plate by femtosecond laser ablation," Journal of Physics 59, 666 – 669 (2007)
[30] Jaeggi, B., Cangueiro, L., Bruneel, D., Ramos de Campos, J.A., Neuenschwander, B., Micromachining using pulse bursts: Influence of the pulse duration and the number of pulses in the burst onto the specific removal rate," Proc. of SPIE 10519, 1051905 (2018)
[31] Schmid, M., Zehnder, S., Schwaller, P., Neuenschwander, B., Zuercher, J., Hunziker, U., Measuring the complex refractive index of metals in the solid and the liquid state and its influence on the laser machining," Proc. of SPIE 8607, 86071I (2013)